A01-25358

42nd AIAA/ASME/ASCE/AHS/ASC Structures, Structural Dynamics, and Materials Conference and Exhibit
Seattle, WA 16-19 April 2001

AIAA-2001-1666

AN ADVANCED BUFFET LOAD ALLEVIATION SYSTEM

Jay K. Burnham*, Dale M. Pitt†, Edward V. White†
The Boeing Company
St. Louis, MO

Douglas A. Henderson*
Air Force Research Laboratory
Wright-Patterson AFB, OH

Robert W. Moses*
NASA Langley Research Center
Hampton, VA

Abstract

This paper describes the development of an advanced buffet load alleviation (BLA) system that utilizes distributed piezoelectric actuators in conjunction with an active rudder to reduce the structural dynamic response of the F/A-18 aircraft vertical tails to buffet loads. The BLA system was defined analytically with a detailed finite-element-model of the tail structure and piezoelectric actuators. Oscillatory aerodynamics were included along with a buffet forcing function to complete the aeroservoelastic model of the tail with rudder control surface. Two single-input-single-output (SISO) controllers were designed, one for the active rudder and one for the active piezoelectric actuators. The results from the analytical open and closed loop simulations were used to predict the system performance. The objective of this BLA system is to extend the life of vertical tail structures and decrease their life-cycle costs. This system can be applied to other aircraft designs to address suppression of structural vibrations on military and commercial aircraft.

Nomenclature

A,B,C,D	state space model matrices
A	aerodynamic inertia
B	aerodynamic damping
b	semi-chord
c	control surface, rudder
F_{buf}	buffet forcing function
F_{piezo}	buffet forcing function
g	structural damping
H	transfer function
I	identity matrix
K	generalized stiffness
k	reduced frequency
M	generalized mass
Q	generalized aerodynamic force
s	Laplace variable
t	time
U,u	system input
V	true airspeed
ρ	air density
ω	frequency
φ	modeshape displacement
$q, \ddot{q}$	generalized displacement, acceleration

Introduction

Buffet Background

The capability of modern fighter aircraft to sustain flight at high angles of attack and/or moderate angles of sideslip often results in immersion of part of the aircraft in unsteady, separated, vortical flow emanating from the aircraft's forebody or wings, Figure 1. The flow from these surfaces becomes turbulent and separated when the aircraft is flying at these conditions. This flow contains significant levels of energy over a frequency bandwidth coincident with low-order structural vibration modes of wings, fins, and control surfaces. The induced unsteady pressures that are applied to these lifting surfaces due to the turbulent flow are commonly referred to as buffet. The interaction of the buffet and the structure produces a structural-mode response known as buffeting. Prolonged exposure to the buffet loads has resulted in fatigue of structures on several aircraft. Damage to aircraft due to buffeting has led to redesigns of aircraft structure and increased support costs for the US Air Force and Navy as well as the armed forces of other

* Member, AIAA
† Associate Fellow, AIAA

countries. Time spent inspecting, repairing, and replacing structure impacts the mission availability of the aircraft.

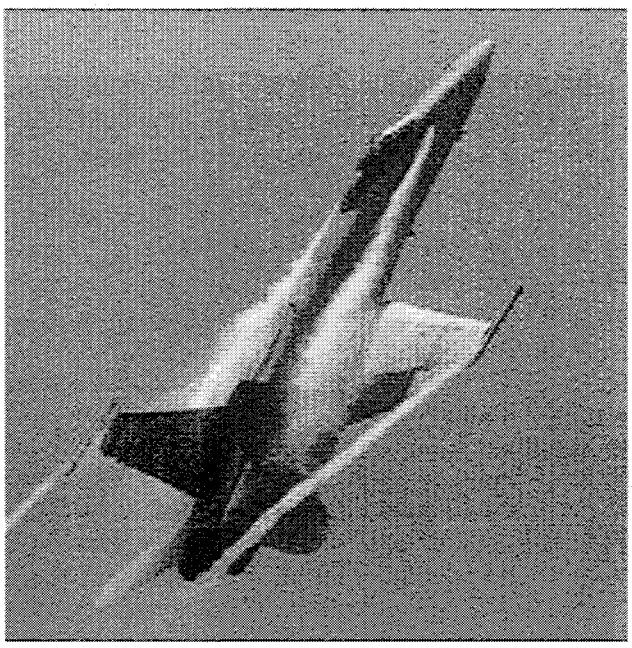

Figure 1. High-Performance Aircraft at High Angle of Attack.

For the F/A-18A-D aircraft, unsteady buffet loads from high angle of attack (20 to 44 degrees) flight impinge on the vertical tails as shown in Figure 1. These buffet loads contribute to the fatigue of the vertical tail structure along with the steady aircraft maneuver loads. The two primary vibration modes that account for the buffet fatigue damage are mode 1, tail 1st bending at ≈15 Hz, and mode 2, tail tip torsion at ≈45 Hz.

Buffet Load Alleviation Background

Several methods have been investigated previously in an effort to reduce the buffet response and increase the fatigue life of vertical tails on military aircraft. One approach to solving this issue was to add passive damping material to the tails while they are being manufactured.[1] Another approach increased the bending stiffness of the tails.[2] The F/A-18A-D aircraft have additional structure added to the vertical tails in conjunction with a fence on the wing leading edge extension (LEX) that disperses the vortex prior to impinging on the vertical tail.[3,4] The additional structure in combination with the LEX fence produces a vertical tail that exceeds the fatigue requirements of the U.S. Navy (6000-hour lifetime). More recently, the F/A-18E/F aircraft has replaced the LEX fence with an actuated spoiler on the LEX. These techniques have been successful at reducing the buffet response of the vertical tails but have increased the cost and gross weight of the vehicle in varying degrees.

Another method to reduce the buffet response incorporated an active control system that deflects the rudder in response to measured motion at the tip of the tail.[5,6] This method increases the fatigue life at most angles of attack through control of mode 1 (F/A-18 vertical tail 1st bending) at 15 Hz. This method is limited to controlling the response of the structural modes within the rudder actuation bandwidth (< 20 Hz on F/A-18A-D aircraft). Therefore, it is not effective for reducing the fatigue damage from mode 2 at 45 Hz (vertical tail tip torsion).

Investigations and tests of active control of the vertical tail vibration response using "smart" materials (piezoelectric actuators) distributed over the vertical tail structure has proven successful at reducing the overall buffet response.[7,8] A full scale test on the F/A-18 vertical tail with a piezoelectric actuator-based active control system was completed during 1997 and 1998 at the International Follow-On Structural Test Program (IFOSTP) facility in Melbourne, Australia.[8] The results from this test indicated that the piezoelectric actuators attached to the skin were more effective at reducing the response of mode 2 (tip torsion at 45 Hz) than mode 1 (1st bending at 15 Hz).

The major problem with using the piezoelectric actuators attached to the tail skin for controlling mode 1 arises from the strain energy distribution for this mode and the stiffness of the tail structure near the root. From the finite element model results, 40% of the modal strain energy for mode 1 is in the root springs of the model that represents the aircraft aft fuselage compliance and 50% of the modal strain energy is in the tail skins. Of this 50%, the majority of the modal strain energy is located near the root of the tail. The piezoelectric actuators are ineffective near the tail root because of the large structural stiffness in this region (skins greater than 0.2 inches thick supported by the tail attachment root rib). In contrast to this, the piezoelectric actuators are very effective for mode 2 because this mode has 60% of the modal strain energy in the tail skins and this strain energy is concentrated in the upper third of the vertical tail where the skin thickness is closer to a tenth of an inch (0.07 to 0.15 inches).

System Design

System Development

The development of the buffet load alleviation (BLA) system for the F/A-18 vertical tail began with research into existing BLA systems to establish a benchmark for system design. Extensive research and testing has been completed in the past ten years on the development of an active BLA system for vertical tails of fighter aircraft as described previously. The results from this research identified two systems that have been effective at actively reducing the buffet response of a vertical tail. The first system employs the rudder control surface to actively control the vertical tail dynamic response[5,6] and the second system utilizes piezoelectric actuators attached to the skin.[7,8] NASA LaRC developed the combination of these two systems under the Scaling Influences Derived from Experimentally Known Impact of Controls (SIDEKIC) program.[9]

The blended system of the rudder and piezoelectric actuator technologies[9] was selected for the design of the F/A-18 vertical tail buffet load alleviation system presented in this paper, Figure 2. The application of this combined system, in which the rudder actuator is used to control the response of the tail mode 1 (1st bending near 15 Hz) and the piezoelectric actuators are used to control mode 2 (tip torsion mode near 45 Hz), uses the most effective features of each system.

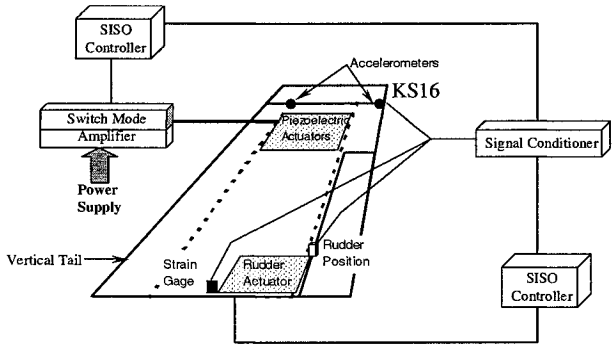

Figure 2 Major Components of BLA System

The major components of the active BLA system are shown in Figure 2. The blended actuator system includes a separate single-input, single-output (SISO) controller for each system. The existing aircraft rudder actuator and servo system is combined with a SISO controller, sensors and signal conditioner to complete the active rudder system. The piezoelectric actuator system is similar except that the switch mode amplifier, which is connected to the aircraft power supply, drives the piezoelectric actuators. Both systems utilize the response of the two accelerometers and strain gage shown in Figure 2. The rudder actuation system includes the rotary variable displacement transducer (RVDT) to provide rudder position feedback.

System Requirements

The objective of the BLA system design is to reduce the buffet response of the F/A-18 vertical tail and extend the operational life of the structure. The BLA system performance goal was established as a 25% reduction in the buffet response at the fatigue critical condition. The fatigue critical condition is not the condition of peak buffet response but is determined from the combination of buffet response and aircraft usage. This combination produces fatigue damage tables, which identify the critical fatigue condition for each vibration mode of the vertical tail.

The analytical performance objective was doubled from 25% to 50% reduction at the fatigue critical condition to account for differences between the analytical representation and the actual hardware of the BLA system.[9] The use of free strain parameters for the piezoelectric actuators leads to over predicting the performance along with unaccounted for losses due to stacking the actuators and the general nonlinear behavior of the piezoelectric actuators.[9] Also, the analytical representation of the rudder aeroservoelastic model tends to over predict the rudder effectiveness.[5] The analytical model can be improved with correlation to measured flight test data.

Technical Approach

The modal equations for aeroelastic response were used to develop a state space representation of the buffet load alleviation (BLA) system, similar to previous research.[5-8] The total degrees of freedom of the structural dynamic equations of motion for a flexible structure are greatly reduced by transforming the equations from physical coordinates, xyz, to modal coordinates, q. Several controllers were designed and analytical simulations were completed to evaluate the BLA system. The modeling tools used at Boeing in the F/A-18 Structural Dynamics group were utilized to complete this task, namely NASTRAN for structural modeling, N5KM (doublet lattice) for aerodynamic modeling[11], FAMUSS for aeroservoelastic modeling[12], MATLAB and SIMULINK for controller design and system simulation.

The starting point for the analysis was with an existing F/A-18 vertical tail structure NASTRAN plate/shell model with root springs for the cantilevered boundary.

The results from a normal modes analysis compared well with measured results. The normal modes analysis in NASTRAN produces vibratory frequencies, ω, and mode shapes, φ.

The unsteady aerodynamics of the vertical tail were represented using a linear doublet lattice computer code, N5KM.[11] The unsteady aerodynamic forces on the tail result from the tail vibratory motion and are not to be confused with the buffet aerodynamic force on the tail. The unsteady aerodynamic forces on the tail are transformed from physical coordinates, xyz, to modal coordinates, q. The NASTRAN vibratory mode shapes, φ, were combined with the unsteady Aerodynamic Influence Coefficient (AIC) to generate generalized aerodynamic forces at a series of reduced frequencies ($k=\omega b/V$; where ω=oscillatory frequency, b=semi-chord, and V=Velocity). These generalized aerodynamic forces were combined with the generalized mass, M, and generalized stiffness, K. Modal damping is expressed as structural damping, g, and is part of the complex stiffness term. The initial equation of motion for the flexible tail in modal coordinates, q(t), is in equation 1.

$$M\ddot{q}(t)+K(1+g\sqrt{j})q(t)=\frac{1}{2}\rho V^2Q(k)q(t) \qquad (1)$$

Equation 1 is solved to assess the aeroelastic stability of the flexible tail. A flutter analysis was completed and the results compared well with the Boeing F/A-18 Project analysis.

The buffet aerodynamic force on the vertical tail was modeled with a similar approach as used in previous research.[8] The buffet force is modeled as a Gaussian white noise process with shaping filters and is applied to the vertical tail model at the same location as the IFOSTP shaker attachment.[8] The shaping filters were scaled to match measured response from flight test data for the six flight conditions analyzed. The unit buffet force, $F_{buf}(t)$, was added to the right hand side of equation 1 to obtain equation 2.

$$M\ddot{q}(t)+K(1+g\sqrt{j})q(t)-\frac{1}{2}\rho V^2Q(k)q(t)=F_{buf}(t) \qquad (2)$$

The modal force from the piezoelectric actuators was determined from the analytical actuation of the piezoelectric elements on the vertical tail model. The model was loaded with a delta temperature across the piezoelectric elements that produced a specified strain in these elements. The resulting grid point forces in the model were multiplied by the corresponding vibration modeshape for each degree-of-freedom to determine the piezoelectric modal force, F_{piezo}. The piezoelectric actuator force was added to the right hand side of equation 2.

$$M\ddot{q}(t)+K(1+g\sqrt{j})q(t)-\frac{1}{2}\rho V^2Q(k)q(t)=F_{buf}(t)+F_{piezo}(t) \qquad (3)$$

The next step was the addition of the aeroservoelastic model for rudder control. Because the vertical tail structural modes are excited by the rudder control surface deflections, the equations of motion were re-written to account for the aircraft control surface deflections. The control surface inertia effects, M_c, and aerodynamic effects, $Q_c(k)$ are included in equation 4 on the right hand side with the commanded system input U(t).

$$\begin{aligned} &M\ddot{q}(t)+K(1+g\sqrt{j})q(t)-\frac{1}{2}\rho V^2Q(k)q(t)= \\ &-M_c\ddot{U}(t)+\frac{1}{2}\rho V^2Q_c(k)U(t)+F_{buf}(t)+F_{piezo}(t) \end{aligned} \qquad (4)$$

The transfer function frequency response of equation 4 was computed from the Laplace transform as given by equation 5. This is the technique used in FAMUSS.[12]

$$\begin{aligned} &\left[Ms^2+K(1+g\sqrt{j})-\frac{1}{2}\rho V^2Q(k)\right]q(s)= \\ &\left[-M_Cs^2+\frac{1}{2}\rho V^2Q_C(k)+F_{buf}+F_{piezo}\right]u(s) \end{aligned} \qquad (5)$$

Equation 5 can be re-written as a transfer function, output/input. The output is the modal coordinates q and the input is u. This produces the modal transfer function response of the modal coordinates for a rudder input, buffet force input, and piezoelectric actuator input, where $s=j\omega$ and $k=\omega b/V$.

$$H_q(s)=\frac{q(s)}{u(s)} \qquad (6)$$

$$\begin{aligned} H_q(s)=&\left[Ms^2+K(1+g\sqrt{j})-\frac{1}{2}\rho V^2Q(k)\right]^{-1}\bullet \\ &\left[-M_Cs^2+\frac{1}{2}\rho V^2Q_C(k)+F_{buf}+F_{piezo}\right] \end{aligned} \qquad (7)$$

The modal transfer function is transformed to the physical coordinate system using the vibratory mode shapes, φ. The transfer function in the physical coordinates is given by equation 8.

$$H(s) = \frac{y(s)}{u(s)} = \frac{\phi_c q(s)}{u(s)} = \phi_c H_q(s) \quad (8)$$

Equation 7 was solved in FAMUSS[12], over the frequency range of interest, 0.5 to 100 Hz. The transfer function is calculated over a series of frequencies, ω, or Laplace variables, s=jω. This process involves interpolating the tabulated unsteady aerodynamic terms of Q(k) and $Q_c(k)$, which are a function of k=ωb/V, over the frequency range of interest, ω. A separate transfer function is calculated for each input-output pair.

The next step in FAMUSS was to create an equivalent state space model that could be used in the subsequent time domain transient analysis, SIMULINK. The state space equations are written as:

$$\begin{aligned} \dot{x}(t) &= A\,x(t) + B\,u(t) \\ y(t) &= C\,x(t) + D\,u(t) \end{aligned} \quad (9)$$

Again, FAMUSS was used to develop an equivalent state space model, equation 9, which matched the original transfer function response, equation 8. The transfer function frequency response for a MIMO state space model is shown in matrix form in equation 10.

$$\hat{H}(s) = C\left[sI - A\right]^{-1} B + D \quad (10)$$

FAMUSS,[12] uses a nonlinear optimization technique to determine the individual terms of the state matrices A, B, C, and D to fit the transfer function response at each tabulated frequency, ω. The resulting aeroservoelastic state space model from FAMUSS had three inputs: 1) rudder rotation, 2) buffet force, and 3) piezoelectric actuator force.

The state space model was incorporated into the MATLAB® SIMULINK toolbox and time history simulations of the vertical tail buffet response were completed. The design of the rudder and piezoelectric controllers were also completed in SIMULINK.

Structure Model

Vertical Tail Structure Model

The F/A-18 vertical tail structure was modeled with a detailed NASTRAN plate/shell finite element model. The detailed model includes the skin elements, spars and ribs. The total weight of the model was 284 lbs. The model is cantilevered with attachment springs along the root to represent the compliance of the aft fuselage. The rudder is modeled along the rudder elastic axis with bar elements and attached to the vertical tail with a rotational spring, which represents the rudder actuator.

The results from the normal modes analysis of the model are listed in Table 1 along with the measured frequencies from a ground vibration test of an F/A-18 aircraft. The analytical-to-measured percent difference in frequency is less than 3% for the buffet critical modes 1 and 2. The modeshapes of the first two modes of the analytical model are displayed in Figure 3

Vert. Tail Mode Description	Analytical Freq. - Hz	Measured Freq. - Hz	Percent Difference
1 - 1st Bending	15.3	15.3	0.0%
2 - Tip Torsion	44.7	46.0	-2.8%
3 - Rudder Rot.	49.6	49.6	0.0%

Table 1 Analytical and Measured Frequency

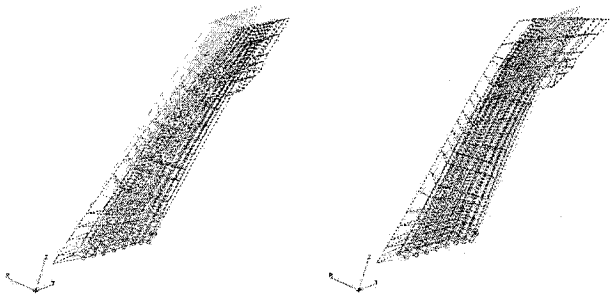

Figure 3 Analytical Modeshape for Modes 1 and 2

Piezoelectric Actuator Model

The first step in modeling the piezoelectric actuators was to determine the vertical tail skin area for attaching the actuators. This was accomplished by using the results from the normal modes analysis along with the restrictions on where actuators can be physically attached to the vertical tail skin. A shaded contour of the strain energy density for Mode 2 is displayed in Figure 4 for the model skin elements. This contour reveals the strain energy is in the upper half of the vertical tail skin and the highest densities are in the upper third. The initial area selected for piezoelectric actuators is also shown in Figure 4.

The candidate piezoelectric actuators for the BLA system could be subdivided into two categories for finite element modeling, 1) isotropic plates (d31 piezoelectric actuation) and 2) orthotropic plates (d33

piezoelectric actuation). The isotropic plates were used to represent the monolithic piezoceramic material with solid plate electrodes that uses the d31 piezoelectric charge constant. The orthotropic plates were used to represent the piezoelectric actuators with interdigitated electrodes (IDE) in lieu of the solid plate electrodes. The IDE creates an electric field along the piezoceramic material to utilize the d33 piezoelectric charge constant. A comparison of the two different piezoelectric actuation mechanisms is shown in Figure 5. The solid line depicts the undeflected shape of the piezoelectric actuator and the dotted line depicts the powered, deflected shape (not to scale) for a fixed voltage polarity. The deflected shapes would change sign for a reversal in voltage polarity. It is important to note that the longitudinal (3 axis) and transverse (2 axis) strains for the IDE actuators are out of phase with each other.

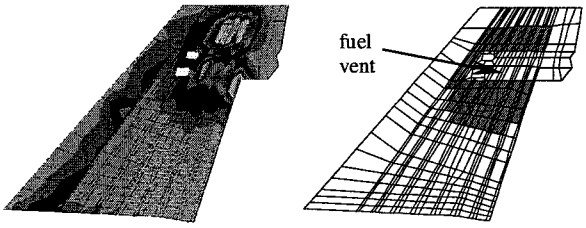

Figure 4 Mode 2 Strain Energy Density and Initial Area for Piezoelectric Actuator Attachment

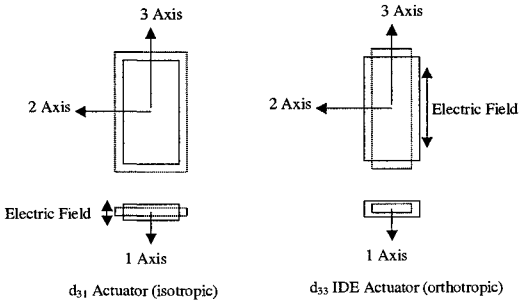

Figure 5 Piezoelectric Actuator d31 (isotropic) and d33 (orthotropic) Mechanisms

The piezoelectric actuators were modeled in NASTRAN as structural plate elements (CQUAD4, PSHELL, MAT1 and MAT8) and were offset from the existing skin elements, similar to previous modeling practices[8,10]. Since the d33 IDE actuators produce directional strain, these actuators were modeled with the orthotropic material MAT8 card. The direction of the principal skin strain for the vertical tail 2nd mode was used to determine the orientation of the piezoelectric d33 IDE axis. The orientation angle was averaged over three application regions.

The analytical actuation of the piezoelectric elements was accomplished using a thermal analogy.[8] The piezoelectric elements had a nonzero coefficient of thermal expansion (CTE) while the rest of the model had a zero CTE. The CTE was determined from the piezoelectric actuator free strain properties at the manufacturer recommended actuation limits. A static solution was performed with the loading of a delta temperature, producing the limit strains in the piezoelectric elements. The results from the static analysis for a d31 isotropic piezoelectric actuator produced a deflected shape similar to the tail first bending mode and the results for a d33 IDE orthotropic actuator produced a shape similar to the 2nd mode, tip torsion. The results from this comparison are significant because the piezoelectric actuators in the BLA system are required to reduce the response of mode 2 and not mode 1. This comparison explains the results found during the BLA system performance analysis, that the d33 IDE actuators out performed the d31 isotropic actuators in mode 2 response.

Aerodynamic Model

Oscillatory Aerodynamics

The dynamic motion of the vertical tail in flight generates oscillatory aerodynamic forces. These forces were included in the BLA equations of motion for the vertical tail and rudder control surface as defined previously in equations 1 and 4. The oscillatory aerodynamic forces were computed using the subsonic Doublet-Lattice Method and the Boeing program N5KM.[11] This is consistent with the current methods used on the Boeing F/A-18 project Structural Dynamics team.

The doublet lattice aerodynamic model was completed for the vertical tail planform with 656 boxes. The flat plate aerodynamic model consisted of 4 panels, two on the vertical tail, one for the rudder and one for the fuselage interference. The model verification was completed by performing a flutter solution (equation 2) at Mach 0.80 and by comparing the results with the Boeing F/A-18 project Structural Dynamics correlated flutter analysis. The detailed BLA model compared well with the existing project analysis. The only major difference between the two solutions was the damping for mode 2, tip torsion. This difference can be attributed to the two structural models, detailed plate FEM for the BLA analysis versus an elastic axis beam

for the project analysis. The detailed FEM produces chordwise bending for increased aerodynamic forces in the tip torsion mode as compared to the rigid chord representation of the beam model.

Buffet Aerodynamics

The buffet aerodynamic force was modeled with a Gaussian white noise process and shaping filter to match the response of measured flight test data.[8] The measured flight test data used for selecting the analysis conditions and scaling the buffet force was obtained from the Boeing F/A-18 project Structural Dynamics database. As described previously, the primary buffet aerodynamic force from flight originates from the wing leading edge extension (LEX) and impinges on the vertical tail as shown in Figure 1. This buffet aerodynamic excitation has been successfully simulated in the full scale ground test facility (IFOSTP) in Melbourne Austrailia.[8] Because of this and the probability of future testing of BLA systems at the IFOSTP facility, the buffet aerodynamic force for the BLA system was analytically modeled as a point force coinciding with the IFOSTP shaker attachment location, intersection of the vertical tail mid-rib and 46% spar.[8] The buffet force of unit magnitude was added to the BLA system equations of motion as an input quantity varying with time, $F_{buf}(t)$ as shown previously in equation 2.

The Boeing F/A-18 project Structural Dynamic database was queried to select the flight test conditions for analysis of the BLA system. The fatigue damage of the F/A-18 vertical tail is based on the band-pass filtered response for mode 1 (10-20 Hz) and mode 2 (32-52 Hz) of the vertical tail aft-tip accelerometer KS16,[3,4] shown in Figure 2. Therefore, the flight test conditions for analysis were based on the measured flight test response of this same parameter, KS16.

The final step in defining the buffet aerodynamic force was to run "open loop" analytical simulations of the BLA system in SIMULINK as described previously. The buffet force analytical shaping filters were scaled to produce the G's RMS response from the measured flight test data. A final check was completed by computing the frequency response of the simulated time history for KS16 and by comparing this to the measured frequency response. Based on these results, the final adjustments were made to the buffet force shaping filters.

Aeroservoelastic Model

The analytical aeroservoelastic model of the BLA system was created in FAMUSS[12], which is the tool used for the F18 aircraft aeroservoelastic analysis. The inputs to FAMUSS include the terms listed in equation 4. The left hand (lh) side of equation 4 includes the structural mass, stiffness, damping, and oscillatory aerodynamic force from the motion of the flexible tail. The right hand (rh) side of equation 4 includes the commanded rudder inertia and oscillatory aerodynamic force, along with the buffet aerodynamic force and piezoelectric actuator force. These three forces on the rh side of equation 4 represent the inputs to the aeroservoelastic model as described previously. The subsequent transfer function analysis and state space model development are described in the Technical Approach, equations 6-10. For the open and closed loop analysis in SIMULINK, the analytical rudder actuator model from the Boeing F18 project was included to complete the rudder control model. The rudder actuator model represents the commanded input and output of the rudder hydraulic actuator.

$$M\ddot{q}(t) + K(1+g\sqrt{j})q(t) - \frac{1}{2}\rho V^2 Q(k)q(t) = -M_c\ddot{U}(t) + \frac{1}{2}\rho V^2 Q_c(k)U(t) + F_{buf}(t) + F_{piezo}(t) \quad (4)$$

Additional analyses were completed in FAMUSS to verify the vertical tail response and commanded rudder sign convention. With only commanded rudder inertia force on the rh side of equation 4, $-M_c\ddot{U}(t)$, the rudder response from the lh side of equation 4 is in phase and the tail response is out of phase with the commanded rudder. Similarly, with only commanded rudder aerodynamic force on the rh side of equation 4, $0.5*\rho V^2 Q_c(k)U(t)$, the lh side rudder response and vertical tail response are out of phase with the commanded rudder. A plot of commanded rudder force and its two components, inertia and aero, versus frequency revealed the crossover frequency is about 7 Hz. For frequencies less than 7 Hz, the aerodynamic component comprises the majority of the commanded rudder force and for frequencies above 7 Hz, the commanded rudder inertia force dominates. Because the active rudder is used to control the tail first bending mode at 15 Hz and at this frequency, the commanded rudder aerodynamic force is small compared to the inertia force, the rudder aerodynamic effectiveness was not reduced as done in previous work.[5]

Model Verification

The completed aeroservoelastic model was validated by comparison of the analytical results with measured results from the full scale ground test at IFOSTP[8], measured aircraft buffet flight test response[4], and measured aircraft response from a commanded rudder frequency sweep on the NASA Dryden F-18 HARV aircraft.

To validate the buffet force model, the analytical state space model without aerodynamics was forced in SIMULINK with the measured shaker load cell time history from the full scale IFOSTP ground test.[8] The analytical model with a structural damping of 8% compared well with the measured vertical tail response at IFOSTP.

The oscillatory aerodynamic force was validated by comparison with measured buffet flight test response of the F18 vertical tail.[4] The analytical state space model poles of frequency and damping were compared with the measured frequency and damping from flight for several buffet flight conditions. The analytical and measured results agreed well for mode 2, tip torsion at 45 Hz. The results for mode 1 indicated the oscillatory aerodynamic force was low and could be increased to account for the increased aerodynamic force on the first bending mode at high angle of attack, which increases the spanwise flow across the tail.

The rudder control surface aeroservoelastic model was validated by comparison with the measured response from an in-flight rudder sweep on the F/A-18 HARV aircraft. In order to get good agreement with the measured results, the analytical rudder response in SIMULINK was changed to include the commanded response (lh side of equation 4) added to the flexible response (rh side of equation 4). Response transfer functions computed from this total rudder position in the denominator agreed well with the measured transfer functions.

Controller Design

The classical control laws were developed independently as single-input, single-output (SISO) for the rudder to control mode 1 at 15 Hz and the piezoelectric actuators to control mode 2 at 45 Hz. The feedback sensor for each control law was selected as the vertical tail aft tip acceleration (KS16 in Figure 2) because it is used to assess fatigue damage of the vertical tail. The control law development was completed in MATLAB with the aeroservoelastic state space model.

After evaluating several different controller designs for the rudder, the best performance was obtained from the simple feedback controller of displacement as shown in Figure 6. The commanded rudder position is determined from the feedback of KS16 acceleration response multiplied by $1/s^2$ to yield displacement and multiplied by 400 for gain.

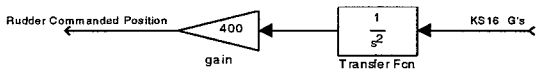

Figure 6 Rudder Feedback Control

Similarly, the best performing controller for the piezoelectric actuators is shown in Figure 7, which is a simple feedback control of velocity from KS16 in conjunction with a notch filter and voltage saturation limit. The notch filter frequency is near 15 Hz to remove the feedback response of mode 1 for the piezoelectric actuators.

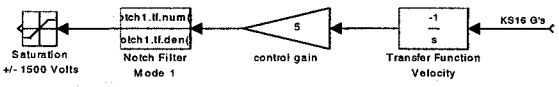

Figure 7 Piezoelectric Actuator Feedback Control

BLA System Performance

The complete analytical model of the BLA system was incorporated into the MATLAB SIMULINK toolbox where both open and closed loop time history simulations were completed to determine the system performance. Several different piezoelectric actuator types and configurations were evaluated. The d33 IDE actuators out performed the d31 isotropic actuators in reducing the mode 2 response while staying within the manufacturer voltage range limits. This result was expected because an analytical actuation of the d33 actuators produces a similar response to mode 2 and an actuation of the d31 actuators produces a response similar to mode 1 as described previously.

Open and closed loop analyses for the piezoelectric actuator control of mode 2 was completed first. The results from the open and closed loop response at the critical fatigue condition are in Figure 8. An additional result from the piezoelectric control was the reduction in response of the tail 2nd torsion mode around 93 Hz.

A plot of the commanded piezoelectric actuator voltage is included in the lower half of Figure 8. The performance objective of 50% reduction in Mode 2 response was met using the NASA LaRC MFC actuators[13] (d33 IDE) over an area of 538 in^2 (269 in^2 X 2 sides) and with an active piezoelectric material thickness of 0.060 inches. This equates to a total actuator weight of about 10 lbs. The piezoelectric actuator attachment area is shown in Figure 4 as the shaded region above the notched void (fuel vent, strobe light, and antenna). A voltage range limit of ±1500 volts was used for this analysis, which is well within the manufacturer limit of ±2000 volts. The 0.060 inch thickness was established from the maximum thickness used during the previous IFOSTP ground test[8] and represents the stacking of 3 layers of 0.020 inch actuators. Similar results could be obtained by halving the actuator thickness to 0.030 inches and by doubling the application area to include 600 in^2 (2 X 300 in^2 per side) of area below the fuel vent, Figure 4.

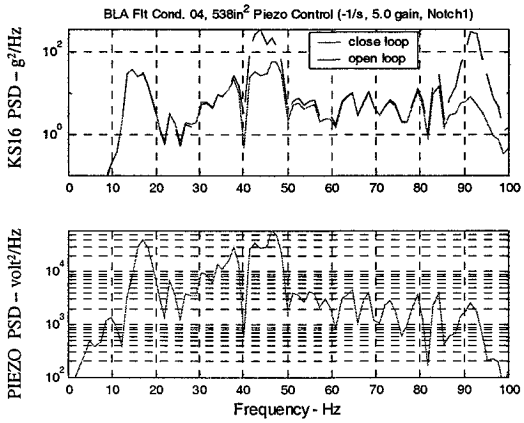

Figure 8 Open/Closed Loop Piezo Control

The results from the open and closed loop response at the critical condition for rudder actuator control of mode 1 are in Figure 9. A plot of the commanded rudder position is included at the bottom of Figure 9. The performance objective of 50% reduction in mode 1 response was accomplished with a maximum of ±2 degrees of commanded rudder. Because of the rudder inertia response to the commanded rudder position, the maximum rudder response was ±3.6 degrees for ±2 degrees of commanded input.

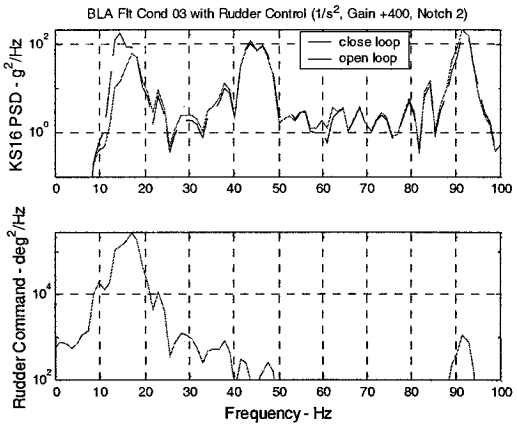

Figure 9 Open/Closed Loop Rudder Control

The final analysis was completed with both the piezoelectric and rudder actuator control systems active. The performance from the combined condition was better than the individual conditions because of the improved isolation for each feedback controller. The results for the critical mode 2 condition with combined control are in Figure 10. Also included at the bottom of this figure are the commanded inputs for the piezoelectric (top) and rudder (bottom). The overall performance of the combined feedback control system produced 70% to 30% vertical tail buffet response reductions for flight conditions ranging from moderate to severe buffet. This was accomplished with a maximum commanded rudder position of ±2 degrees (15 Hz) and about 10 lbs of piezoelectric actuators operating at a peak power level of 2000 watts.

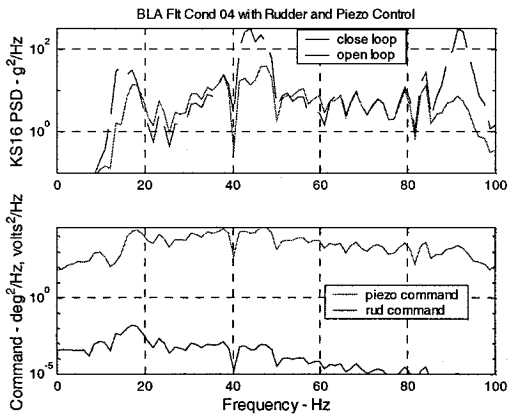

Figure 10 Open/Closed Loop Piezo-Rudder Control

Conclusions

The development of an advanced buffet load alleviation (BLA) system for use on the F-18 vertical tail has been completed. The BLA system uses the most effective features of two systems, the rudder actuator and control surface are used to control the response of the tail first bending mode near 15 Hz, and piezoelectric actuators are used to control the response of the second tail mode, tip torsion, near 45 Hz. The analytical aeroservoelastic model was validated by good agreement with measured results from a full scale ground test,[8] measured aircraft buffet flight test response,[4] and an in-flight commanded rudder frequency sweep.

The overall performance of the BLA system produced 70% to 30% vertical tail buffet response reductions for flight conditions ranging from moderate to severe buffet. This was accomplished with a maximum commanded rudder position of ±2 degrees (15 Hz) and about 10 lbs of piezoelectric actuators attached to the vertical tail skin and operating at a peak power level of 2000 watts. By meeting the design objective, this system would extend the vertical tail fatigue life beyond two aircraft lifetimes. This system is also adaptable to other aircraft surfaces and vehicle platforms.

Acknowledgement

This work was primarily accomplished under the research and development contract, F33615-95-D-3216, between the USAF Research Laboratory, Wright Patterson AFB and the Boeing Company.

References

1. Liguore, S., Ferman, M., and Yurkovich, R., "Integral damping treatment for primary aircraft structures," Damping '91 Conference, San Diego, CA, 13-15 February 1991.

2. Ferman, M. A., et al., "Composite `Exoskin' Doubler Extends F-15 Vertical Tail Fatigue Life," AIAA Paper 93-1341.

3. Scanlon, R.W.., "F/A-18 Vertical Tail/LEX Fence Dynamic Response Wind Tunnel Test Program," Boeing Co. Report MDC B1393, 31 January 1989.

4. Levesque, G. S., "F/A-18 Vertical Tail/LEX Fence Dynamic Response Flight Test Program," Boeing Co. Report MDC B1430, 1 March 1989.

5. Ashley, H., Rock, H., Digumarthi, R., Chaney, K., and Eggers, A., "Active control for fin buffet alleviation," United States Air Force Research Laboratory Report WL-TR-93-3099, January 1994.

6. Pado, L E. and Lichtenwalner, P. F., "Neural Predictive Control for Active Buffet Alleviation," AIAA-99-1319, 40th AIAA Structures, Structural Dynamics, and Materials Conference, St. Louis, MO, 12-15 April 1999.

7. Moses, R. W., "Vertical Tail Buffeting Alleviation Using Piezoelectric Actuators – Some Results of the Actively Controlled Response of Buffet-Affected Tails (ACROBAT) Program," SPIE's 4th Annual Symposium on Smart Structures and Materials, Industrial and Commercial Applications of Smart Structures Technologies Conference, San Diego, CA, 4-6 Mar 97.

8. Spangler, R. L., "An Active Smart Material System for Buffet Load Alleviation," United States Air Force Research Laboratory Report AFRL-VA-WP-TR-1998-3079, November 1998.

9. Moses, R. W., "Contributions to Active Buffeting Alleviation Programs by the NASA Langley Research Center," 40th AIAA Structures, Structural Dynamics, and Materials Conference, St. Louis, MO, 12-15 April 1999.

10. Barmac, T.K., and Campbell, J.F., "Non-Linear Finite Element Modeling of THUNDER Piezoelectric Actuators", SPIE Conference on Smart Structures and Integrated Systems, Newport Beach, CA, Mar 99.

11. Kalman, T.P., Giesing, J.P,., Subsonic Steady and Oscillatory Aerodynamics for Multiple Interfering Wings and Bodies, Boeing Report MDC-J7295, Volume I, Oct. 1976.

12. Pitt, D.M., and Goodman, C.E., FAMUSS: A New Aeroservoelastic Modeling Tool, AIAA Paper 92-2395.

13. Wilkie, W.K., et al, "Low-Cost Piezocomposite Actuator for Structural Control Applications", SPIE 7th International Symposium on Smart Structures and Materials, Newport Beach, CA, March 5-9, 2000.